Journal of Chemical&Engineering Data

pubs.acs.org/jced

Article

Reverse Pluronic 10R5-Based Aqueous Biphasic Systems with Ammonium Salts: A Novel Platform for Phenolic Compound Partitioning

Published as part of Journal of Chemical & Engineering Data special issue "Aqueous Two-Phase Systems for Separation Processes: From Fundamental Data to Applications".

Silvia J. R. Vargas, Thaís S. Soares, Filipe H. B. Sosa, and Maria C. Hespanhol*

Cite This: J. Chem. Eng. Data 2025, 70, 3332−3343

Read Online

ABSTRACT: The valorization of lignocellulosic biomass is essential for developing sustainable bioprocesses and producing high-value compounds such as phenolics. However, the efficient separation of these compounds remains challenging due to their structural diversity. This study explored the use of aqueous biphasic systems (ABS) composed of poly(propylene glycol)-*block*-poly(ethylene glycol)-*block*-poly(propylene glycol), Pluronic 10R5, and different biodegradable ammonium salts (acetate, tartrate, and citrate) for the extraction of phenolic compounds. Phase diagrams were constructed at three temperatures (289.2, 298.2, and 313.2 K) and characterized by the binodal curve, tie-line length, and slope of the tie-line, with phase inversion phenomena observed for the first time in reverse Pluronic-based systems. The system with ammonium citrate exhibited the best performance in terms of extraction efficiency, biodegradability, and pH compatibility, resulting in stable phenolic compound stability. Five model compounds were evaluated, yielding partition coefficients ranging from 3.5 to 6.5 and extractions exceeding 80% in the polymer-rich phase. These findings demonstrate the potential of sustainable ABS as an effective platform for selective recovery processes in lignocellulosic biorefineries.

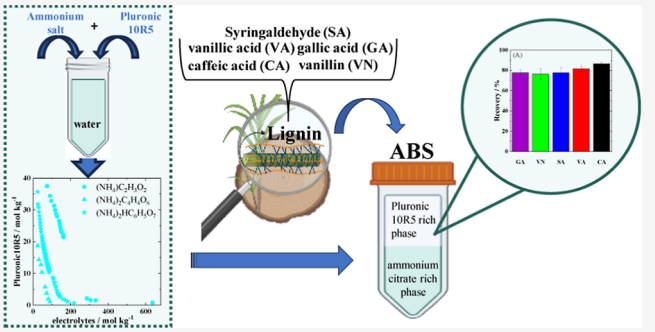

1. INTRODUCTION

Aqueous biphasic systems (ABSs) are liquid−liquid extraction platforms formed by the phase separation of two water-soluble components, such as polymers, salts, and ionic liquids, among others,[1−7] under specific concentration and temperature conditions. Each phase is enriched in one of the constituents and exhibits distinct physicochemical properties,[7,8] making ABS a versatile media for separation, purification, and preconcentration processes.[6,9] Due to their high water content, low volatility, and biocompatible components, ABSs are widely regarded as more sustainable alternatives to conventional organic solvent-based extraction systems, generally resulting in reduced environmental impact.

The versatility of ABSs lies in the tunability of their phase properties through variation in the type and concentration of phase-forming components. The most extensively reported systems combine polymers and salts, with polyethylene glycol (PEG) being one of the most commonly used polymers.[2,10−24] Although these systems exhibit good separation efficiencies and several applications, they are limited to analytes with a more hydrophilic character,[25−28] as this polymer possesses high hydrophilicity.

To modulate the hydrophilic/hydrophobic character of biphasic systems more effectively, triblock copolymers have begun to be used as forming components of these systems.[1,3,20,29−31] Triblock copolymer, prominently exemplified by Pluronic, constitutes a material produced by the arrangement of hydrophilic and hydrophobic segments. The poly(propylene oxide) (PO) units impart more hydrophobic characteristics to the copolymer, as they have one more methyl group than the poly(ethylene oxide) (EO) units. Thus, the amount and proportion of EO and PO units, as well as the order of these units in the organization of the copolymer, help shape its hydrophobicity.[32] When the structural organization of the blocks follows the order $(EO)_x-(PO)_y-(EO)_x$, the

Received: May 1, 2025
Revised: June 23, 2025
Accepted: July 10, 2025
Published: July 16, 2025

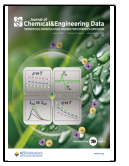

https://doi.org/10.1021/acs.jced.5c00298
J. Chem. Eng. Data 2025, 70, 3332−3343

Table 1. List of Chemicals and of Their Suppliers, Purities, CAS Numbers and Abbreviations

chemical	supplier	mass fraction purity[a]	CAS	abbreviation[b]
poly(propylene glycol)-*block*-poly(ethylene glycol)-*block*-poly(propylene glycol), ~2000 g·mol^{-1}	Sigma-Aldrich	≥0.990	9003-11-6	Pluronic 10R5
ammonium tartrate dibasic ($(NH_4)_2C_4H_4O_6$)	Sigma-Aldrich	≥0.980	3164-29-2	ammonium tartrate
ammonium acetate ($NH_4C_2H_3O_2$)	Vetec	≥0.970	631-61-8	ammonium acetate
ammonium citrate dibasic ($(NH_4)_2HC_6H_5O_7$)	Synth	≥0.980	3012-65-5	ammonium citrate
vanillin ($C_8H_8O_3$)	Sigma-Aldrich	≥0.990	121-33-5	VN
vanillic acid ($C_8H_8O_4$)	Sigma-Aldrich	≥0.970	121-34-6	VA
syringaldehyde ($C_9H_{10}O_4$)	Sigma-Aldrich	≥0.980	134-96-3	SA
caffeic acid ($C_9H_8O_4$)	Sigma-Aldrich	≥0.980	331-39-5	CA
gallic acid ($C_7H_6O_5.H_2O$)	Riedel-deHäen	≥0.980	5995-86-8	GA

[a]Purities are reported as provided by the suppliers. [b]Names correspond to the names used in the text.

copolymer is called normal, and when the order is $(PO)_x$–$(EO)_y$–$(PO)_x$, the copolymer is known as reversed.[33]

While triblock copolymers of the Pluronic normal family have been widely studied for ABS formation due to their biocompatibility and negligible toxicity,[1,29,31,34−38] their applications extend beyond extraction to fields such as controlled drug delivery,[38] nanotechnology,[39] bioengineering,[40] and metallurgy.[41,42] However, a less explored subset of this family, known as reverse Pluronic or Pluronic-R, exhibits unique properties that have not been extensively studied, suggesting significant potential for novel applications To the best of our knowledge, the use of reverse Pluronic (Pluronic-R) in the formation of ABSs remains limited,[20,25,43,44] and their influence on the partitioning behavior of strategic compounds has been scarcely explored. No studies have specifically examined how phenolic compounds are distributed in these systems. In addition, liquid−liquid equilibrium data with organic ammonium electrolytes are rare despite these salts being environmentally safe and compatible with different analytical techniques.

To address the identified knowledge gap, this study investigates the formation and phase behavior of ABSs composed of the reverse triblock copolymer Pluronic 10R5 and three organic ammonium salts—acetate, citrate, and tartrate—at 283.15, 298.15, and 313.15 K. Phase diagrams were constructed to elucidate the binodal curves and tie-line compositions, providing comprehensive equilibrium data for these underexplored systems. To assess the separation potential of these systems, five phenolic compounds—gallic acid, caffeic acid, vanillin, vanillic acid, and syringaldehyde—were selected as model solutes. These molecules are structurally diverse and have been identified as key products in biomass,[45−48] coal liquefaction oil,[47,49,50] as well as coal tar and petroleum.[51,52] Furthermore, liquid−liquid equilibrium (LLE) modeling was performed using the NRTL equation to assess the scalability of these systems for industrial implementation. These insights contribute to the rational design of sustainable and efficient separation processes, addressing current limitations in biorefinery strategies.

2. EXPERIMENTAL AND/OR COMPUTATIONAL METHODS

2.1. Chemicals. The reagents used in this study are listed in Table 1, along with their suppliers, purity levels, CAS numbers, and abbreviations. All reagents were of analytical grade and were used without further purification or pretreatment. The construction of the aqueous systems involved the use of Pluronic 10R5 copolymer—a poly(propylene glycol)-*block*-poly(ethylene glycol)-*block*-poly(propylene glycol) triblock with an average molar mass of approximately 2000 and an ethylene oxide content of 50% (w/w)—as well as ammonium tartrate, ammonium acetate, and ammonium citrate dibasic. Vanillin, vanillic acid, syringaldehyde, caffeic acid, and gallic acid were used as target analytes in the partition experiments. All solutions were prepared using ultrapure water with a resistivity of 18.25 MΩ·cm at 298 K, obtained from a Milli-Q Gradient purification system (Millipore). All chemicals were used as received without additional purification.

2.2. Binodal Curve. The turbidimetric titration method[47] was employed to determine the binodal curve at 283.2, 298.2, and 313.2 K. For this purpose, aqueous stock solutions of 50% (w/w) ammonium acetate, 46% (w/w) ammonium citrate, 15% (w/w) ammonium tartrate, and 86% (w/w) Pluronic 10R5 were initially prepared. At each studied temperature, 0.500 g of the Pluronic 10R5 solution was introduced into a glass tube, followed by the gradual addition of the ammonium salt solution (acetate, citrate, or tartrate) until phase separation was visually detected, indicating the onset of biphasic system formation. Subsequently, water was added to the tube until the solution regained transparency. The masses of salt and water required to induce and reverse turbidity were recorded, and this procedure was repeated multiple times to ensure sufficient data for constructing the binodal curve.

The experimental data were then plotted and fitted using the empirical model proposed by Merchuk et al.[48] described by the following equation

$$Y = A \exp(BX^{0.5} - CX^3) \quad (1)$$

where X and Y represent the mass fractions of salt and macromolecule, respectively, while A, B, and C are adjustable parameters obtained through nonlinear regression of the experimental data.

All measurements were conducted using a high-precision analytical balance (Shimadzu AG 220, accuracy ± 0.0001 g) and a thermostatic water bath (Microquímica MQBTC 99−20, uncertainty ± 0.1 K) to ensure reliable and reproducible results.

2.3. Determination of Phase Diagrams. Merchuk et al.[48] proposed the gravimetric method to determine the phase diagrams of the systems investigated in this study. Ternary mixtures were prepared in syringes by accurately weighing appropriate masses of Pluronic 10R5, ammonium salt (acetate,

https://doi.org/10.1021/acs.jced.5c00298
J. Chem. Eng. Data 2025, 70, 3332−3343

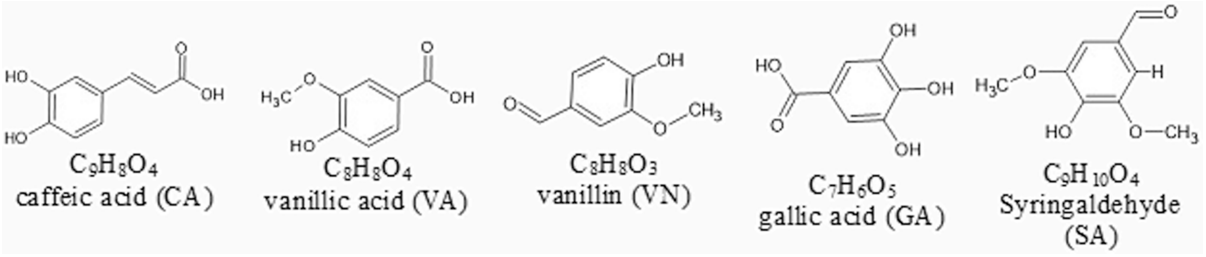

Figure 1. Chemical structure and molecular formula of the phenolic compounds analyzed in this study.

Table 2. Liquid−Liquid Equilibrium Data and TLL, in % (w/w), for the Pluronic 10R5 (w_1) + Ammonium Citrate Dibasic (w_2) + H_2O (w_3) System at Different Temperatures and Pressure of 0.10 MPa[a]

overall			macromolecule-rich phase			electrolyte-rich phase				
$100w_1$	$100w_2$	$100w_3$	$100w_1$	$100w_2$	$100w_3$	$100w_1$	$100w_2$	$100w_3$	100TLL	STL
					283.2 K					
25.43	22.14	52.43	60.49	7.00	32.51	10.44	28.61	60.95	54.51	−2.32
29.13	23.84	47.03	79.17	2.88	17.95	4.34	34.22	61.44	81.14	−2.39
31.28	24.77	43.95	86.53	1.88	11.59	2.77	36.57	60.66	90.66	−2.41
32.79	25.42	41.79	92.12	1.29	6.59	2.11	37.90	59.99	97.17	−2.46
33.84	25.92	40.24	93.80	1.26	4.94	1.43	39.26	59.31	99.89	−2.43
					298.2 K					
25.43	22.15	52.42	64.95	5.88	29.17	9.22	28.83	61.95	60.27	−2.43
29.18	23.87	46.95	75.13	4.52	20.35	5.24	33.94	60.82	75.83	−2.38
33.48	25.07	41.45	89.38	3.12	7.50	3.66	36.79	59.55	92.09	−2.55
35.60	25.82	38.58	92.27	2.91	4.82	3.03	38.99	57.98	96.26	−2.47
37.57	26.56	35.87	94.92	2.72	2.36	2.45	41.16	56.39	100.1	−2.41
					313.2 K					
26.00	21.44	52.56	60.00	4.72	35.28	0.01	34.22	65.77	66.85	−2.03
29.18	23.86	46.96	68.31	3.19	28.50	0.01	39.32	60.67	77.26	−1.89
32.82	25.44	41.74	75.26	2.13	22.61	0.01	43.46	56.53	85.85	−1.82
36.20	27.00	36.80	86.37	1.07	12.56	0.01	45.60	54.39	97.17	−1.94
37.51	28.14	34.35	89.26	1.07	9.67	0.01	47.76	52.23	100.73	−1.91

[a]Standard errors (u): $u(T)$ = 0.1 K; $u(p)$ = 0.20 kPa; $u(w_1^{ERP})$ = 0.01; $u(w_1^{MRP})$ = 0.19; $u(w_2^{ERP})$ = 0.42; $u(w_2^{MRP})$ = 0.32; $u(w_3^{ERP})$ = 0.32; $u(w_3^{MRP})$ = 0.57; u(TLL) = 0.22; u(STL) = 0.15.

citrate, or tartrate), and water to achieve a final system mass of 4.00 g with a predetermined global composition. The syringes were then sealed, thoroughly mixed, and left to equilibrate in a thermostatic bath at a fixed temperature of 283.2, 298.2, or 313.2 K for 72 h to ensure thermodynamic equilibrium between the phases. For each ABS, four different global compositions were prepared in duplicate.

After the 72 h equilibration period, the electrolyte-rich phase (m^{ERP}) was carefully collected by slowly depressing the plunger of the syringe and weighed. The mass of the macromolecule-rich phase (m^{MRP}) was determined using a mass balance approach, given that the total system mass (m_{total}) was known, as shown in eq 2

$$m^{MRP} = m_{total} - m^{ERP} \tag{2}$$

The phase compositions were determined by solving four eqs (eqs 3−6) using Wolfram Mathematica 8.

$$Y_{MRP} = A \times [(B \times X_{MRP}^{0.5}) - (C \times X_{MRP}^{3})] \tag{3}$$

$$Y_{ERP} = A \times [(B \times X_{ERP}^{0.5}) - (C \times X_{ERP}^{3})] \tag{4}$$

$$Y_{MRP} = \frac{Y_M}{\alpha} - \frac{1-\alpha}{\alpha} Y_{ERP} \tag{5}$$

$$X_{MRP} = \frac{X_M}{\alpha} - \frac{1-\alpha}{\alpha} X_{ERP} \tag{6}$$

In this system, Y_{MRP}, Y_{ERP}, and Y_M represent the mass fractions of the macromolecule (Pluronic 10R5) in the macromolecule-rich phase (MRP), the electrolyte-rich phase (ERP), and the total ABS mass, respectively. Likewise, X_{MRP}, X_{ERP}, and X_M denote the mass fractions of ammonium salt in the MRP, ERP, and the total ABS mass, respectively. The parameter α corresponds to the ratio between the MRP and total system mass. A, B, and C are regression parameters derived from fitting the experimental data.

Tie-line length (TLL) and tie-line length slope (STL) for the different ABS were determined according to eqs 7 and 8, respectively

$$TLL = [(C_M^{MRP} - C_M^{ERP})^2 + (C_E^{MRP} - C_E^{ERP})^2]^{0.5} \tag{7}$$

$$STL = \frac{C_M^{MRP} - C_M^{ERP}}{C_E^{MRP} - C_E^{ERP}} \tag{8}$$

where C_M^{MRP} and C_M^{ERP} represent the concentrations of the macromolecule in the macromolecule-rich phase (MRP) and electrolyte-rich phase (ERP), respectively, while C_E^{MRP} and C_E^{ERP} denote the concentrations of salt in the MRP and ERP, respectively.

https://doi.org/10.1021/acs.jced.5c00298
J. Chem. Eng. Data 2025, 70, 3332−3343

Table 3. Liquid−Liquid Equilibrium Data and TLL, in % (w/w), for the Pluronic 10R5 (w_1) + Ammonium Acetate (w_2) + H_2O (w_3) System at Different Temperatures and Pressure of 0.10 MPa[a]

overall			macromolecule-rich phase			electrolyte-rich phase				
$100w_1$	$100w_2$	$100w_3$	$100w_1$	$100w_2$	$100w_3$	$100w_1$	$100w_2$	$100w_3$	100TLL	STL
					283.2 K					
30.86	23.11	46.03	50.83	16.40	32.77	5.10	31.76	63.14	48.24	−2.98
32.53	23.86	43.61	58.40	14.13	27.47	1.84	35.45	62.71	60.45	−2.65
					298.2 K					
25.82	18.93	55.25	41.58	12.61	45.81	0.24	29.29	70.47	44.58	−2.48
28.43	20.62	50.95	53.22	10.34	36.44	0.03	32.40	67.57	57.58	−2.41
30.81	22.22	46.97	54.91	9.99	35.10	0.01	37.87	62.12	61.57	−1.97
32.51	23.86	43.63	61.56	8.60	29.84	0.01	40.94	59.05	69.53	−1.90
37.28	27.06	35.66	62.77	8.33	28.90	0.01	54.49	45.50	77.91	−1.36
					313.2 K					
30.54	21.85	47.61	49.48	7.87	42.65	0.01	44.40	55.59	61.50	−1.35
32.84	23.28	43.88	51.23	7.70	41.07	0.01	51.13	48.86	67.15	−1.18
33.82	24.24	41.94	51.29	7.39	41.32	0.01	51.92	48.07	70.31	−1.22
35.35	25.32	39.33	56.65	7.17	36.18	0.01	55.46	44.53	74.43	−1.77
36.39	26.16	37.45	59.59	6.87	33.54	0.01	56.43	43.56	77.49	−1.20

[a]Standard errors (u): $u(T)$ = 0.1 K; $u(p)$ = 0.20 kPa; $u(w_1^{ERP})$ = 0.11; $u(w_1^{MRP})$ = 0.47; $u(w_2^{ERP})$ = 0.42; $u(w_2^{MRP})$ = 0.37; $u(w_3^{ERP})$ = 0.42; $u(w_3^{MRP})$ = 0.67; u(TLL) = 0.18; u(STL) = 0.11.

Table 4. Liquid−Liquid Equilibrium Data and TLL, in % (w/w), for the Pluronic 10R5 (w_1) + Ammonium Tartrate (w_2) + H_2O (w_3) System at Different Temperatures and Pressure of 0.10 MPa[a]

overall			macromolecule-rich phase			electrolyte-rich phase				
$100w_1$	$100w_2$	$100w_3$	$100w_1$	$100w_2$	$100w_3$	$100w_1$	$100w_2$	$100w_3$	100TLL	STL
					283.2 K					
25.47	16.02	58.51	42.79	6.01	51.20	8.80	25.65	65.55	39.26	−1.73
26.55	17.01	56.44	46.27	5.32	48.41	7.01	28.61	64.38	45.65	−1.69
27.40	17.88	54.72	48.19	4.98	46.83	5.60	31.41	62.99	50.13	−1.61
28.02	18.47	53.51	49.60	4.74	45.66	4.80	33.25	61.95	53.11	−1.57
29.16	19.29	51.55	52.27	4.32	43.41	3.89	35.67	60.44	57.65	−1.54
					298.2 K					
18.39	9.40	72.21	28.67	6.20	65.13	10.56	11.85	77.59	18.97	−3.21
18.79	9.84	71.37	33.70	4.88	61.42	5.18	14.37	80.45	30.06	−3.01
18.97	10.21	70.82	34.38	4.71	60.91	2.99	15.92	81.09	33.33	−2.80
19.54	10.64	69.82	36.85	4.13	59.02	1.62	17.39	80.99	37.64	−2.66
19.97	11.14	68.89	37.36	4.01	58.63	0.73	19.04	80.23	39.59	−2.44
					313.2 K					
22.95	13.59	63.46	37.03	4.99	57.98	0.01	27.62	72.38	43.39	−1.64
24.69	15.13	60.18	39.81	4.64	55.55	0.01	32.28	67.72	48.46	−1.44
26.28	16.71	57.01	42.39	4.33	53.28	0.01	36.92	63.08	53.46	−1.30
29.68	19.91	50.41	48.07	3.66	48.27	0.01	45.70	54.30	63.85	−1.14
32.40	21.82	45.78	53.74	3.03	43.23	0.01	50.34	49.66	71.59	−1.14

[a]Standard errors (u): $u(T)$ = 0.1 K; $u(p)$ = 0.20 kPa; $u(w_1^{ERP})$ = 0.16; $u(w_1^{MRP})$ = 0.37; $u(w_2^{ERP})$ = 0.42; $u(w_2^{MRP})$ = 0.45; $u(w_3^{ERP})$ = 0.57; $u(w_3^{MRP})$ = 0.50; u(TLL) = 0.37; u(STL) = 0.35.

2.4. Modeling Using the NRTL. The liquid−liquid equilibrium (LLE) data of all ABS were correlated using the non-random two-liquid (NRTL) model, which accounts for local composition effects and is suitable for partially miscible systems. In this work, the NRTL model was employed in its mass fraction-based form with temperature-dependent interaction parameters to calculate activity coefficients, as previously reported in the literature.[49] The model parameters were estimated using the Fortran-based TML-LLE 2.0 code, which applies the Simplex optimization method in conjunction with the maximum likelihood principle.[50] The correlation quality was evaluated through the root-mean-square deviation (RMSD) between the experimental and calculated compositions.

2.5. Partition of Phenolic Compounds. In this study, vanillin (VN), vanillic acid (VA), syringaldehyde (SA), gallic acid (GA), and caffeic acid (CA) were selected as model molecules to evaluate the partitioning of phenolic compounds (Figure 1).

Biphasic systems were prepared by combining Pluronic 10R5, ammonium citrate dibasic, water, and an aqueous solution of each analyte in defined proportions. The mixtures were assembled in 4.5 mL polypropylene tubes with screw caps, ensuring that each system contained 2 g of the top phase and 2 g of the bottom phase. The overall system composition corresponded to the first tie-line (60.27), as indicated by the equilibrium data presented in Table 2.

https://doi.org/10.1021/acs.jced.5c00298
J. Chem. Eng. Data 2025, 70, 3332−3343

After preparation, the systems were stirred until they became turbid and then incubated in a thermostatic bath at 298.2 K for at least 24 h, allowing the formation of well-defined phases with a limpid interface. Once thermodynamic equilibrium was reached, the top and bottom phases were carefully separated and collected. Finally, the pH of both phases was determined using pH indicator strips.

Final concentrations were varied from 25 to 100 mg kg^{-1} to assess potential differences in the partitioning or extraction behavior of each analyte in the biphasic system consisting of Pluronic 10R5, ammonium acetate, and water at 298.2 K. The analyte concentration in the bottom phase was determined using ultraviolet−visible (UV−vis) spectrophotometry with a UV−vis spectrometer (Shimadzu UV-2550 digital double beam spectrometer).

An individual calibration curve was constructed for each analyte using an external standard, with solutions prepared in deionized water at concentrations ranging from 2.5 to 40 mg kg^{-1}. Spectrophotometric measurements were performed at a specific wavelength for each compound: 279 nm for vanillin, 252 nm for vanillic acid, 306 nm for syringaldehyde, 263 nm for gallic acid, and 286 nm for caffeic acid.

Two parameters were determined to evaluate the partitioning performance of each phenolic compound: the partition coefficient (K_D) and the extraction percentage to Pluronic 10R5-rich phase (%E_{MRP}). Specific abbreviations were used to differentiate the partition coefficients of each phenol compound (Figure 1): K_{CA},K_{VA},K_{VN},K_{GA},K_{SA}. The concentration of each compound in the electrolyte-rich phase (C_{ERP}) was determined using UV−vis spectrophotometry. Meanwhile, the concentration in the macromolecule-rich phase (C_{MRP}) was estimated by mass balance. Based on these data, the distribution coefficient (K_D) and the %E_{MRP} were calculated according to eqs 9 and 10, respectively. Each experiment was performed in triplicate to ensure data accuracy and reproducibility.

$$K_D = \frac{C_{MRP}}{C_{ERP}} \tag{9}$$

$$\% E_{MRP} = \frac{n_{MRP}}{n_{total}} \times 100 \tag{10}$$

where n_{MRP} represents the mass of each phenolic compound in the macromolecule-rich phase, and n_{total} is the total mass of each compound in the system.

3. RESULTS AND DISCUSSION

3.1. Equilibrium Data of Aqueous Biphasic Systems. Tables 2−4 show the phase composition, tie-line length, and slope of biphasic systems formed by Pluronic 10R5 + $(NH_4)_2C_6H_6O_7$ + H_2O, Pluronic 10R5 + $NH_4C_2H_3O_2$ + H_2O, and Pluronic 10R5 + $(NH_4)_2C_4H_4O_6$ + H_2O, respectively, at 283.2, 298.2, and 313.2 K. The standard uncertainties were determined based on a quantitative characterization of phase distribution, considering the composition of the macromolecule-rich phase and the electrolyte-rich phase at all three temperatures. The phase composition data were expressed in mass percent—% (w/w). Table S1 summarizes the parameters obtained from fitting the experimental data using the empirical equation proposed by Merchuk to describe the behavior of aqueous two-phase systems.

The knowledge of equilibrium data in liquid−liquid systems designed for extracting, separating, or partitioning strategic solutes is essential for optimizing experimental conditions and maximizing process efficiency. It also supports the development of predictive models that generalize the behavior of similar systems. However, inverse Pluronic-based systems, such as Pluronic 10R5, have been less extensively studied[43−46] compared to conventional Pluronic systems, resulting in a limited understanding of phase partitioning mechanisms in these systems and their potential application in selective separation processes. This study aims to expand the equilibrium data available for inverse Pluronic-based systems, enhancing understanding of their phase partitioning behavior and potential for selective separation processes.

The tie-line length defines the equilibrium phase compositions in ABSs at constant temperature, pressure, and concentration, quantifying the compositional contrast between the electrolyte-rich and macromolecule-rich phases. This parameter is essential for modeling solute partitioning and evaluating phase separation efficiency. The experimentally determined TLL and STL values are summarized in Tables 2−4 Results show that TLL increases with global composition, consistent with polymer-salt ABS trends. The phase behavior of Pluronic 10R5 closely follows reported equilibrium data, indicating that its higher hydrophobicity does not significantly alter its phase formation relative to less hydrophobic copolymers or conventional polymers in aqueous saline systems.[46]

3.2. Influence of the Nature of Anion on the Binodal Curve. The influence of anion nature on the binodal curve position was analyzed in ABS formed by Pluronic 10R5 at the three studied temperatures with three different ammonium salts. The mass fractions of the electrolytes ($(NH_4)C_2H_3O_2$, $(NH_4)_2C_4H_4O_6$, $(NH_4)_2C_6H_5O_7$) and Pluronic 10R5 were normalized by dividing by their respective molar masses (w_i/M_i) to enable a consistent comparison among salts with different molecular weights. Since molar masses (M_i) were expressed in kg mol^{-1}, the values of w_i/M_i were reported in mol kg^{-1}. Since all the salts employed shared the same cation (NH_4^+), the differences observed in the behavior of the biphasic systems are attributed solely to the nature of the anion.

Figure 2 illustrates the variation in the binodal curve position for the three electrolytes with different anionic structures ($C_4H_4O_6^{2-}$, $C_6H_6O_7^{2-}$, $C_2H_3O_2^-$) at 298.2 K. The binodal curves at 283.2 and 313.2 K are shown in Figure S1. All experimental data corresponding to the binodal curves obtained in this study are provided in Tables S3−S5.

Experimental results reveal that the biphasic region expands in the following order: $C_4H_4O_6^{2-}$ > $C_6H_6O_7^{2-}$ > C_2H_3O, suggesting that lower concentrations of divalent anions are sufficient to induce phase separation. This trend aligns with the kosmotropic nature of multivalent organic anions, as predicted by the extended Hofmeister series,[51,52] anions such as tartrate and citrate, characterized by their high hydration capacity and polyfunctional structures, facilitate micellar dehydration and promote the establishment of two-phase systems.[53] Interestingly, although the Hofmeister series predicts a greater salting-out effect for citrate than for tartrate, our data show a larger biphasic region for tartrate. This discrepancy may be attributed to the more complex molecular architecture of citrate, which could hinder its interaction with the hydrophobic domains of the copolymer due to steric and conformational constraints.[54]

https://doi.org/10.1021/acs.jced.5c00298
J. Chem. Eng. Data 2025, 70, 3332−3343

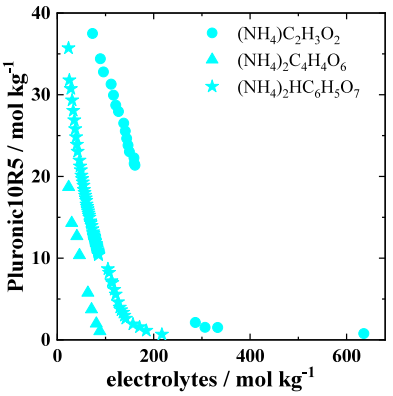

Figure 2. Influence of nature of anion on the binodal curve Pluronic 10R5 + ammonium electrolyte + H_2O at 298.2 K. $NH_4C_2H_3O_2$: ammonium acetate; $(NH_4)_2C_4H_4O_6$: ammonium tartrate; $(NH_4)_2HC_6H_5O_7$: ammonium citrate dibasic.

These observations are in agreement with previous reports involving ammonium-based salts in ABS formed with hydrophobic polymers such as PPG425[55] as well as with Pluronic L35, a block copolymer with similar molecular weight and poly(ethylene oxide) (PEO) content.[31] Comparable phase behavior has also been reported for these ammonium-based salts in aqueous systems containing Pluronic L64, a less hydrophobic block copolymer composed of approximately 40 wt % poly(ethylene oxide) (PEO).[56] Despite extensive investigations, a unified mechanistic understanding of phase separation in polymer−salt ABS remains elusive.[57−61] This lack of consensus highlights the complexity of the interactions governing liquid−liquid phase separation. Given the analogous phase behavior observed in copolymer−salt systems, it is plausible that similar entropic and ion-specific mechanisms—particularly those involving preferential hydration and polymer conformation—also play a dominant role. Nonetheless, additional experimental data involving block copolymers with varying hydrophobicity, coupled with calorimetric and spectroscopic characterization, are essential to test this hypothesis rigorously.

3.3. Effect of the Temperature on ABS Composition. Figure 3 presents the experimental binodal curve for all the systems at the three studied temperatures. In all investigations, experimental results indicate that in ABS composed of Pluronic 10R5 and ammonium organic salts, the biphasic area increases when the temperature increases from 283.2 to 313.2 K. Previous studies have shown that the phase separation critical temperature (T_c) of Pluronic 10R5 decreases with structural and chemical modifications, suggesting that heat-induced dehydration of hydrophobic segments plays a key role in phase formation.[62,63] Increasing the temperature alone could drive the expansion of the biphasic domain in these systems. Similar results have been reported for systems composed of Pluronic 10R5 with sodium or potassium citrate and water,[45] as well as for Pluronic 10R5−DES systems.[44] However, additional thermodynamic studies are necessary, as similar behavior is observed in systems with less hydrophobic copolymers.[31,64]

Although the binodal curves partially overlap in some regions, a closer inspection—particularly of the ammonium acetate system—reveals that the curve at 313.2 K is notably more concave, reflecting a larger biphasic region than at 283.2 K. In the cases of ammonium tartrate and citrate, the

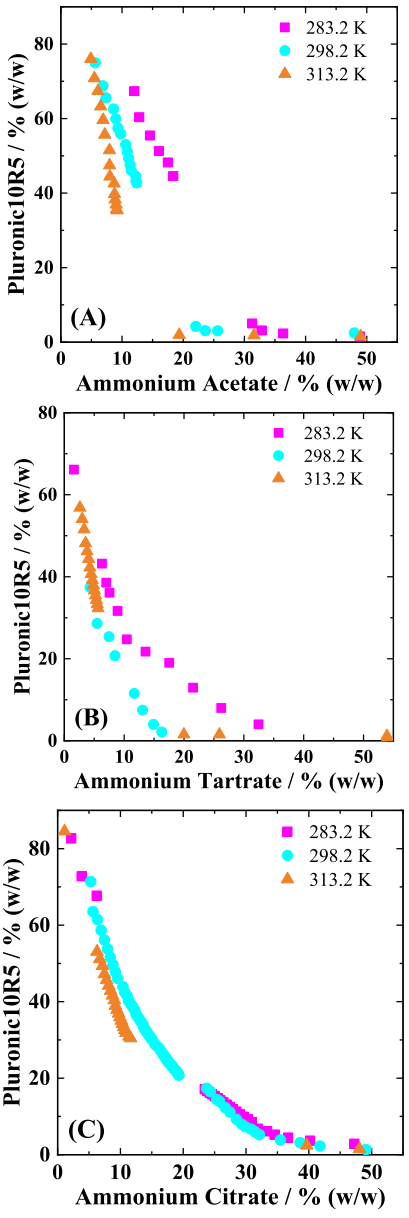

Figure 3. Effect of temperature on the binodal curves of the Pluronic 10R5 + H_2O + ammonium electrolyte systems: (A) ammonium citrate, (B) ammonium tartrate, and (C) ammonium acetate. Experimental data were obtained at 283.2 K (pink ■), 298.2 K (blue ●), and 313.2 K (orange ▲).

expansion of the biphasic area is less visually apparent due to the superposition of experimental points; however, the data points corresponding to 313.2 K (orange markers) consistently shift to the left of those at 283.2 K (pink markers), indicating that phase separation occurs at lower salt concentrations as temperature increases. This behavior supports the inference that temperature promotes biphasic domain expansion in all systems studied.

3.4. Phase Inversion Behavior in ABS Formed with Pluronic 10R5. The phenomenon of phase inversion has been previously reported in ABS, which is composed of copolymers and salts.[56,65] This inversion typically results in the upper phase being enriched in the electrolyte while the lower phase becomes enriched in the macromolecule. However, this phenomenon is often overlooked or not explicitly addressed

https://doi.org/10.1021/acs.jced.5c00298
J. Chem. Eng. Data 2025, 70, 3332−3343

in the literature.[33] likely because most equilibrium diagrams have been studied at salt concentrations already high enough to promote phase inversion. Only a few studies involving copolymers[56,65] have described how, at low concentrations of salt and copolymer, the macromolecule-rich phase initially forms the bottom phase, and the salt-rich phase appears at the top. As the salt concentration increases beyond a certain threshold, a reversal in partitioning occurs: the copolymer migrates to the lower phase, and the salt accumulates in the upper phase—this is known as the phase inversion process. This phenomenon has been scarcely explored in ABS formed with Pluronic, and, to the best of our knowledge, no previous reports exist on Pluronic 10R5-based systems showing noninverted phase behavior. Interestingly, our experimental results revealed that phase inversion only was observed in the Pluronic 10R5 + ammonium acetate + water system.

Figure 4 presents the tie-line length in the system Pluronic 10R5 + $NH_4C_2H_3O_2$ + H_2O at 283.2, 298.2, and 313.2 K. While Figures S2 and S3 present the TLL curve for the Pluronic 10R5 + $(NH_4)_2C_4H_4O_6$ + H_2O and Pluronic 10R5 + $(NH_4)_2C_6H_6O_7$ + H_2O systems at all three temperatures, respectively. To enhance reader comprehension, compositions with phase inversion are highlighted in symbol open and black line, whereas those exhibiting no phase inversion are color-coded according to temperature. As shown in Figure 4, all TLLs for the biphasic systems at 289.2 K exhibited phase inversion. At 298.2 K, phase inversion occurred in the first four TLLs. In contrast, at 313.2 K, only the first TLL showed phase inversion, while the subsequent ones did not. Overall, phase inversion was observed primarily at lower salt concentrations and became progressively less frequent as the salt concentration increased, especially at higher temperatures.

The few studies that have explored phase inversion suggest that it is driven by an increase in the density of the electrolyte-rich phase as the salt concentration increases.[65,66] The phase densities of the Pluronic 10R5 + $NH_4C_2H_3O_2$ + H_2O system at 283.2, 298.2, and 313.2 K are presented in Table S2. Figure 5A–C display the variation in phase density as a function of total salt concentration for the systems at 283.2, 298.2, and 313.2 K, respectively.

In Figure 5A, it is evident that, for the only two tie-line compositions that formed biphasic systems at 283.2 K, phase inversion occurred—both at electrolyte concentrations below 24% (w/w). Similarly, at 298.2 K, phase inversion was observed in the first four tie-lines, which also corresponded to electrolyte overall concentrations below 24% (w/w). At 313.2 K, phase inversion occurred only in the first tie-line, which was associated with a salt concentration below 23% (w/w).

These results indicate that as the salt concentration increases, the system progressively transitions to typical biphasic behavior, where the top phase is rich in macromolecule, and the bottom phase is rich in electrolyte. This transition point is marked by the intersection of the density curves shown clearly in Figure 5B,C.

In contrast, at 283.2 K (Figure 5A), biphasic systems could not be obtained at higher salt concentrations, which prevented the observation of a phase density crossover.

It is the first time such behavior has been reported for ABSs formed with Pluronic 10R5 and inorganic ammonium salts. These findings support the hypothesis that phase inversion is driven by relative density differences between the coexisting

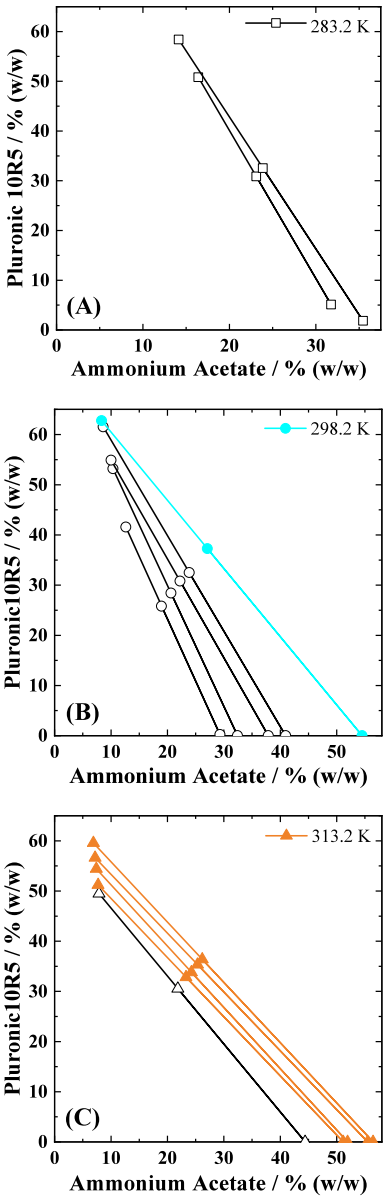

Figure 4. Tie-line length for the Pluronic 10R5 + $NH_4C_2H_3O_2$ + H_2O at 283.2 K (□), 298.2 K (blue ●), 313.2 K (orange▲). Black tie-lines represent systems with phase inversion, while colored tie-lines indicate compositions without phase inversion.

phases, in line with previous observations in systems involving other copolymers.[65]

The different behavior observed in Figure 5 between 298.2 and 313.2 K arises from the thermoresponsive nature of Pluronic 10R5.[67] At higher temperature (313.2 K), dehydration of the PPO blocks leads to stronger micellization and phase separation, resulting in a slightly lower or stable density of the polymer-rich phase due to reduced water and salt content. At 298.2 K, the polymer remains more hydrated, allowing for greater salt and water retention, which initially increases the density before decreasing to higher salt concentrations. The salt-rich phase consistently exhibits an increasing density with increasing salt concentration, as expected due to the accumulation of electrolytes. In contrast, the systems composed of $(NH_4)_2C_4H_4O_6$ and $(NH_4)_2C_6H_5O_7$ exhibited typical behavior reported for most copolymer–salt ABS, where phase inversion is not consistently observed. The

https://doi.org/10.1021/acs.jced.5c00298
J. Chem. Eng. Data 2025, 70, 3332–3343

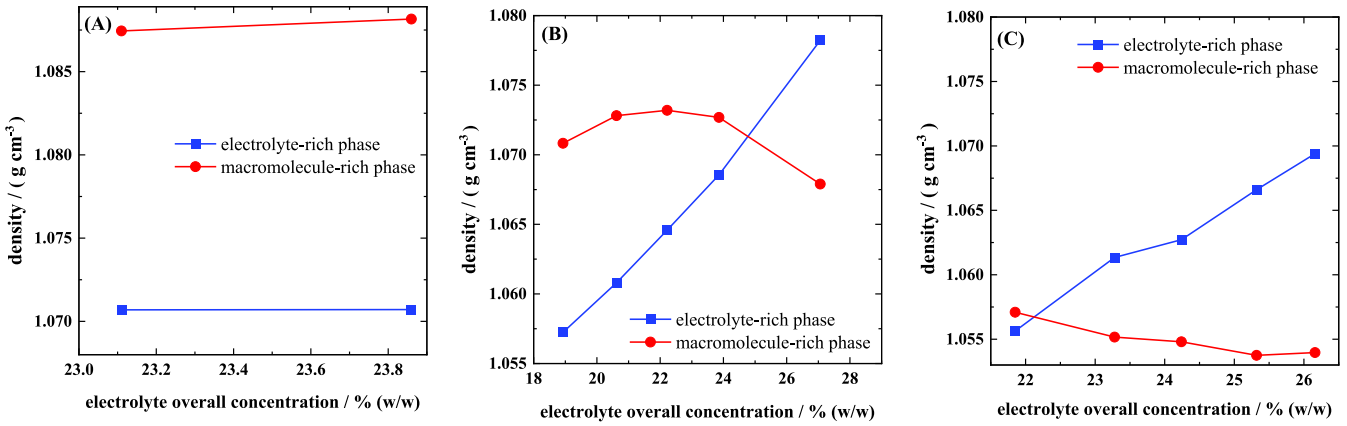

Figure 5. Densities of the polymer-rich (red ●) and salt-rich (blue ■) phases at different salt concentrations in the Pluronic 10R5 + $NH_4C_2H_3O_2$ + H_2O system at 283.2 K (A), 298.2 K (B), and 313.2 K (C).

Table 5. Binary Interaction Parameters of the NRTL Equation and Correlation Performance for the Studied System[a]

i/j	A_{0ij}/K	A_{0ji}/K	A_{1ij}	A_{ji}	$\alpha_{ij} = \alpha_{ji}$	RMSD/%
$NH_4C_2H_3O_2$−Pluronic 10R5	3191.8	70.2	−2.7588	0.7556	0.4700	1.96
$NH_4C_2H_3O_2$−water	97.0	−2539.9	−2.0058	13.0750	0.2000	
Pluronic 10R5−water	−94.8	8999.1	−0.2094	0.0029	0.4072	
$(NH_4)_2C_6H_6O_7$−Pluronic 10R5	−1502.0	2739.2	9.1796	−1.3646	0.3199	3.70
$(NH_4)_2C_6H_6O_7$−water	1092.8	−1195.2	1.1018	30.5150	0.4366	
Pluronic 10R55−water	−1235.7	9025.2	5.7497	−0.0898	0.4299	
$(NH_4)_2C_4H_4O_6$−Pluronic 10R5	1417.0	6757.4	2.0328	−2.8318	0.2258	3.19
$(NH_4)_2C_4H_4O_6$−water	−545.3	5253.4	0.2048	8.8999	0.3135	
Pluronic 10R5−water	−577.6	7817.1	−2.8295	1.3352	0.4700	

[a] $A_{ij} = A_{0ij} + A_{1ij}\,T$ and $A_{ji} = A_{0ji} + A_{1ji}\,T$.

corresponding TLL graphics are provided in Figures S2 and S3.

3.5. Modeling Experimental Liquid−Liquid Equilibrium Using NRTL. The modeling of experimental LLE data is an initial step toward applying these systems on an industrial scale. The application of ABS for partitioning biomolecules in the context of biorefineries requires models that may be able to describe the systems for using simulation software to optimize new processes and unit operations. The LLE modeling involves the activity coefficient calculation, which in this study was calculated using the nonrandom two-liquid model (NRTL) proposed by Renon and Prausnitz.[67]

Liquid−liquid equilibrium correlation was performed using the estimated molecular energy interaction parameters using the Fortran TML-LLE 2.0 Code[50] as described by Sosa et al.[49] Mean squared deviations (RMSD) were calculated according to the following equation

$$\delta_x = 100 \times \sqrt{\frac{\sum_i^M \sum_j^N \left(x_{ij}^{\mathrm{I.exp}} - x_{ij}^{\mathrm{I.calc}}\right)^2 + \left(x_{ij}^{\mathrm{II.exp}} - x_{ij}^{\mathrm{II.calc}}\right)^2}{2MN}} \tag{11}$$

As seen in Table 5 and Figure S4, the NRTL model was able to represent the phase division across the entire range of compositions and temperatures for all systems studied, presenting an RMSD value < 3.70%. These results show that the NRTL model is suitable to represent the phase behavior of the ABS addressed in this work in all temperature ranges 283.2−313.2 K.

3.6. Evaluation of Partition of Phenolic Compounds. The initial screening of the three developed ABSs indicated that the combination of Pluronic 10R5, ammonium citrate dibasic, and water showed the highest potential for recovering phenolic compounds. This system was selected as the most promising candidate because citrate is more cost-effective than other commonly used salts, such as tartrate and acetate, and is biodegradable and nontoxic.[68] These attributes have led to its selection in previous studies for ABS formation, and it has also proven effective in the extraction of phenolic compounds.[68,69]

Previous studies have shown that the stability of phenolic compounds is highly dependent on their chemical structure and the pH of the medium, among other factors. Friedman and Jürgens[70] demonstrated that pH-induced alterations in phenolic compounds are irreversible. Similarly, Lapidot[71] showed that the antioxidant activity of phenolic compounds is maintained across a pH range of 1−8. Based on these findings, the pH values of the equilibrium phases in the tested systems were determined. The systems based on acetate and tartrate exhibited near-neutral pH values (6.5−7.0 and 5.0−7.0, respectively). In contrast, the citrate-based system showed values of 3.3 and 5.3 in the salt-rich and polymer-rich phases, respectively. These results indicate that, even without buffering agents, this system can potentially preserve the chemical integrity of the target phenolic compounds and their bioactivity.

Partition and extraction assays in the polymer-rich phase were conducted using the Pluronic 10R5 + $(NH_4)_2C_6H_5O_7$ + H_2O system, with a global composition of 25.43% Pluronic 10R5, 22.15% ammonium citrate dibasic, and 52.42% water (corresponding to first tie-line length). Concentrations ranging

https://doi.org/10.1021/acs.jced.5c00298
J. Chem. Eng. Data 2025, 70, 3332−3343

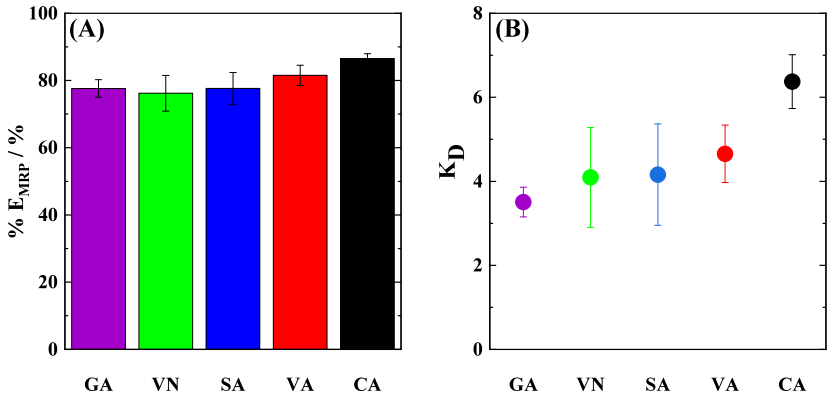

Figure 6. (A) Extraction percentage (%E_{MRP})of phenolic compounds and (B) partition coefficient (K_D) of the phenolic compounds in the system Pluronic 10R5 + $(NH_4)_2C_6H_5O_7$ + H_2O at 298.2 K. Gallic acid (GA), vanillin (VN), syringaldehyde (SA), vanillic acid (VA), and caffeic acid (CA).

from 25 to 100 mg kg^{-1} of each of the five model phenolic compounds were added to evaluate potential changes in extraction capacity due to phase saturation and alterations in the partition coefficient caused by interactions among the analytes at higher concentrations.

Figure 6 displays the extraction percentage in the polymer-rich phase and the partition coefficients of the phenolic compounds under the conditions investigated. All phenolic compounds evaluated exhibited %E_{MRP} close to 80% in the polymer-rich phase, with partition coefficients ranging from 3.5 to 6.5, indicating a clear preferential affinity for this phase. Although no prior data exist on the partition behavior of phenolic compounds in inverted Pluronic systems, their preference for polymer-rich phases—particularly those composed of PEG—has been extensively reported.[14,24,68,69,72,73]

This behavior in polymer-based systems can be explained by a combination of factors, such as hydrophobic interactions and hydrogen bonding between phenolic compounds and the phase-forming polymers, as well as the influence of excluded volume effects, salting-out mechanisms, and the polarity contrast between coexisting phases.[68,74−78]

Similarly, micellar systems formed by Pluronic copolymers in water or other solvents have been used successfully to recover phenolic and other bioactive compounds with greater hydrophobicity, and similar partitioning mechanisms have been proposed to describe their behavior.[79,80] Nevertheless, further studies are needed using copolymer-based systems—particularly those incorporating more hydrophobic Pluronic types such as Pluronic-R—to determine whether structural differences among copolymers significantly influence separation performance.

4. CONCLUSIONS

Reverse Pluronic-based ABS composed of Pluronic 10R5 and ammonium organic salts (acetate, tartrate, and citrate) were investigated for their ability to extract phenolic compounds. A systematic study of their phase behavior, including binodal curves, tie-line lengths, and densities, demonstrated that the nature of the anion significantly influences the biphasic region and phase inversion phenomena. The tartrate anion induced a larger biphasic region, while the acetate anion induced phase inversion. The phase inversion phenomena for Pluronic 10R5-ammonium acetate ABS further enhances understanding of reverse Pluronic-based systems, providing novel insights. The influence of temperature on micellization and phase separation was also confirmed, revealing the thermoresponsive behavior of the system.

The partitioning of five structurally related phenolic compounds (vanillin, vanillic acid, syringaldehyde, gallic acid, and caffeic acid) was evaluated in all ABS proposed. The Pluronic 10R5 + ammonium citrate + water system exhibited the most favorable extraction performance. These results highlight the crucial role of electrolyte composition and pH in determining the phase affinity of phenolic compounds. In particular, the acidic pH of the citrate-based system contributed to maintaining the chemical integrity and potential bioactivity of the target compounds.

Finally, the liquid−liquid equilibrium data of the studied systems were successfully modeled using the NRTL thermodynamic approach, with low deviation values, reinforcing the applicability of this model for the design and optimization of polymer−salt-based ABS. This study expands the understanding of phase behavior in inverse Pluronic-based systems and supports their use as effective extraction platforms for phenolic compounds.

■ ASSOCIATED CONTENT

Supporting Information

The Supporting Information is available free of charge at https://pubs.acs.org/doi/10.1021/acs.jced.5c00298.

Experimental details include Merchuk's equation parameters, density values, experimental data and NRTL model parameters, a binodal curve, and tie-line length (PDF)

■ AUTHOR INFORMATION

Corresponding Author

Maria C. Hespanhol − *Group of Analysis and Education for Sustainability (GAES), Chemistry Department, Centre of Exact and Technology Sciences, Federal University of Viçosa (UFV), Viçosa 36570-900, Brazil;* orcid.org/0000-0003-2296-4516; Email: mariacarmo@ufv.br

Authors

Silvia J. R. Vargas − *Department of Animal Sciences, Purdue University, West Lafayette, Indiana 47907-2041, United States; Group of Analysis and Education for Sustainability (GAES), Chemistry Department, Centre of Exact and Technology Sciences, Federal University of Viçosa (UFV), Viçosa 36570-900, Brazil*

https://doi.org/10.1021/acs.jced.5c00298
J. Chem. Eng. Data 2025, 70, 3332−3343

Thaís S. Soares − *Group of Analysis and Education for Sustainability (GAES), Chemistry Department, Centre of Exact and Technology Sciences, Federal University of Viçosa (UFV), Viçosa 36570-900, Brazil*

Filipe H. B. Sosa − *CICECO - Aveiro Institute of Materials, Department of Chemistry, University of Aveiro, Aveiro 3810-193, Portugal;* orcid.org/0000-0003-1649-4597

Complete contact information is available at: https://pubs.acs.org/10.1021/acs.jced.5c00298

Author Contributions

S.J.R.V.: Conceptualization, data curation, formal analysis, investigation, methodology, writing—original draft, writing—review and editing. T.S.S.: Data curation, formal analysis, investigation, methodology, validation. F.H.B.S. Data curation, formal analysis, writing − original draft. M.C.H. Conceptualization, supervision, visualization, project administration, resources, writing − review and editing.

Funding

The Article Processing Charge for the publication of this research was funded by the Coordenacao de Aperfeicoamento de Pessoal de Nivel Superior (CAPES), Brazil (ROR identifier: 00x0ma614).

Notes

The authors declare no competing financial interest.

■ ACKNOWLEDGMENTS

This work was supported by Conselho Nacional de Desenvolvimento Científico e Tecnológico, CNPq, [grant number 407799/2022-2], and Fundação de Amparo à Pesquisa do Estado de Minas Gerais, FAPEMIG, [grant numbers APQ-01134-23, APQ-03572-23, and RED-00161-23]. TSS thanks Coordenação de Aperfeiçoamento de Pessoal de Nível Superior, CAPES, for the scholar fellowship [grant number 88887.956518/2024-00]. M.C.H. thanks CNPq for research fellowships [grant numbers 305649/2021-3]. This work was developed within the scope of Project from Aveiro Institute of Materials (CICECO) [grant numbers UIDB/50011/2020, UIDP/50011/2020, and LA/P/0006/2020], Fundação para a Ciência e a Tecnologia, FCT [grant number CEECIND/07209/2022].

■ REFERENCES

(1) Jing, Y.; Guo, Y.; Xia, Q.; Liu, X.; Wang, Y. Catalytic Production of Value-Added Chemicals and Liquid Fuels from Lignocellulosic Biomass. *Chem* **2019**, *5*, 2520.

(2) Naseem, A.; Tabasum, S.; Zia, K. M.; Zuber, M.; Ali, M.; Noreen, A. Lignin-derivatives based polymers, blends and composites: A review. *Int. J. Biol. Macromol.* **2016**, *93*, 296.

(3) Liu, X.; Bouxin, F. P.; Fan, J.; Budarin, V. L.; Hu, C.; Clark, J. H. Recent Advances in the Catalytic Depolymerization of Lignin towards Phenolic Chemicals: A Review. *ChemSusChem* **2020**, *13*, 4296.

(4) Luo, H.; Abu-Omar, M. M. Chemicals From Lignin. *Encyclopedia of Sustainable Technologies*; Elsevier, 2017; 573.

(5) Environmental Protection Agency. *Inventory of U.S. Greenhouse Gas Emissions and Sinks:1990−2022*, 2024, https://www.epa.gov/ghgemissions/inventory-us-greenhouse-gas-emissions-and-sinks.

(6) Haq, I.; Mazumder, P.; Kalamdhad, A. S. Recent advances in removal of lignin from paper industry wastewater and its industrial applications − A review. *Bioresour. Technol.* **2020**, *312*, 123636.

(7) Chio, C.; Sain, M.; Qin, W. Lignin utilization: A review of lignin depolymerization from various aspects. *Renew. Sustain. Energy Rev.* **2019**, *107*, 232.

(8) Constant, S.; Wienk, H. L. J.; Frissen, A. E.; Peinder, P. D.; Boelens, R.; Van Es, D. S.; Grisel, R. J. H.; Weckhuysen, B. M.; Huijgen, W. J. J.; Gosselink, R. J. A.; Bruijnincx, P. C. A. New insights into the structure and composition of technical lignins: a comparative characterisation study. *Green Chem.* **2016**, *18*, 2651.

(9) Fele Žilnik, L.; Jazbinšek, A. Recovery of renewable phenolic fraction from pyrolysis oil. *Sep. Purif. Technol.* **2012**, *86*, 157.

(10) Li, J.; Wang, C.; Yang, Z. Production and separation of phenols from biomass-derived bio-petroleum. *J. Anal. Appl. Pyrolysis* **2010**, *89*, 218.

(11) Wei, Y.; Lei, H.; Wang, L.; Zhu, L.; Zhang, X.; Liu, Y.; Chen, S.; Ahring, B. Liquid-liquid extraction of biomass pyrolysis bio-oil. *Energy Fuels* **2014**, *28*, 1207−1212.

(12) Maggi, R.; Delmon, B. Comparison between 'slow' and 'flash' pyrolysis oils from biomass. *Fuel* **1994**, *73*, 671.

(13) Vigneault, A.; Johnson, D. K.; Chornet, E. Base-catalyzed depolymerization of lignin: Separation of monomers. *Can. J. Chem. Eng.* **2007**, *85*, 906.

(14) Kim, J. S. Production, separation and applications of phenolic-rich bio-oil − A review. *Bioresour. Technol.* **2015**, *178*, 90.

(15) Mantilla, S. V.; Manrique, A. M.; Gauthier-Maradei, P. Methodology for Extraction of Phenolic Compounds of Bio-oil from Agricultural Biomass Wastes. *Waste Biomass Valorization* **2015**, *6*, 371−383.

(16) Gallivan, R. M.; Matschei, P. K. Fractionation of oil obtained by pyrolysis of lignocellulosic materials to recover a phenolic fraction for use in making phenol-formaldehyde resins. U.S. Patent 4209647 A, 1978.

(17) Zhang, N.; Wang, S.; Gibril, M. E.; Kong, F. The copolymer of polyvinyl acetate containing lignin-vinyl acetate monomer: Synthesis and characterization. *Eur. Polym. J.* **2020**, *123*, 109411.

(18) Lavoie, J. M.; Baré, W.; Bilodeau, M. Depolymerization of steam-treated lignin for the production of green chemicals. *Bioresour. Technol.* **2011**, *102*, 4917.

(19) Lu, Y.; Wei, X. Y.; Cao, J. P.; Li, P.; Liu, F. J.; Zhao, Y. P.; Fan, X.; Zhao, W.; Rong, L. C.; Wei, Y. B.; Wang, S. Z.; Zhou, J.; Zong, Z. M. Characterization of a bio-oil from pyrolysis of rice husk by detailed compositional analysis and structural investigation of lignin. *Bioresour. Technol.* **2012**, *116*, 114−119.

(20) Voitl, T.; Rohr, P. R. v. Demonstration of a process for the conversion of kraft lignin into vanillin and methyl vanillate by acidic oxidation in aqueous methanol. *Ind. Eng. Chem. Res.* **2010**, *49*, 520−525.

(21) D Modi, U.; K Ghodadara, V.; M Mitchla, S.; M Lakdawala, M. Advanced Techniques in the Purification of Lignin: Challenges, Methods, and Industrial Applications- A Review. *IJARESM* **2024**, *12*, 1332.

(22) Reverchon, E.; De Marco, I. Supercritical fluid extraction and fractionation of natural matter. *J. Supercrit. Fluids* **2006**, *38*, 146.

(23) Rodrigues, G. D.; Lemos, L. R. d.; Patrício, P. d. R.; Silva, L. H. M. d.; Silva, M. d. C. H. da Aqueous two-phase systems: a new approach for the determination of p-aminophenol. *J. Hazard. Mater.* **2011**, *192*, 292.

(24) Santos, J. H. P. M.; Almeida, M. R.; Martins, C. I. R.; Dias, A. C. R. V.; Freire, M. G.; Coutinho, J. A. P.; Ventura, S. P. M. Separation of phenolic compounds by centrifugal partition chromatography. *Green Chem.* **2018**, *20*, 1906.

(25) Almeida, M. R.; Passos, H.; Pereira, M. M.; Lima, A. S.; Coutinho, J. A. P.; Freire, M. G. Ionic liquids as additives to enhance the extraction of antioxidants in aqueous two-phase systems. *Sep. Purif. Technol.* **2014**, *128*, 1.

(26) Santos, J. H.; e Silva, F. A.; Ventura, S. P. M.; Coutinho, J. A. P.; de Souza, R. L.; Soares, C. M. F.; Lima, A. S. Ionic liquid-based aqueous biphasic systems as a versatile tool for the recovery of antioxidant compounds. *Biotechnol. Prog.* **2015**, *31*, 70.

(27) Xavier, L.; Deive, F. J.; Sanromán, M. A.; Rodríguez, A.; Freire, M. S.; González-Álvarez, J.; Gortáres-Moroyoqui, P.; Ruíz-Cruz, S.; Ulloa, R. G. Increasing the Greenness of Lignocellulosic Biomass

Biorefining Processes by Means of Biocompatible Separation Strategies. *ACS Sustain. Chem. Eng.* **2017**, *5*, 3339.
(28) Edrisi, S.; Bakhshi, H. Separation of polyphenolic compounds from Citrus aurantium L. peel by deep eutectic solvents and their recovery using a new DES-based aqueous two-phase system. *J. Mol. Liq.* **2024**, *402*, 124790.
(29) Cláudio, A. F. M.; Ferreira, A. M.; Freire, C. S. R.; Silvestre, A. J. D.; Freire, M. G.; Coutinho, J. A. P. Optimization of the gallic acid extraction using ionic-liquid-based aqueous two-phase systems. *Sep. Purif. Technol.* **2012**, *97*, 142.
(30) Cláudio, A. F. M.; Freire, M. G.; Freire, C. S. R.; Silvestre, A. J. D.; Coutinho, J. A. P. Extraction of vanillin using ionic-liquid-based aqueous two-phase systems. *Sep. Purif. Technol.* **2010**, *75*, 39.
(31) Veloso, A. C. G.; Patrício, P. R.; Quintão, J. C.; de Carvalho, R. M. M.; da Silva, L. H. M.; Hespanhol, M. C. Phase equilibrium of aqueous two-phase systems composed by L35 triblock copolymer + organic and inorganic ammonium electrolytes + water at 298.2 and 313.2 K. *Fluid Phase Equilib.* **2018**, *469*, 26.
(32) de Andrade, V. M.; Rodrigues, G. D.; de Carvalho, R. M. M.; da Silva, L. H. M.; da Silva, M. C. H. Aqueous two-phase systems of copolymer L64 + organic salt + water: Enthalpic L64−salt interaction and Othmer−Tobias, NRTL and UNIFAC thermodynamic modeling. *Chem. Eng. J.* **2011**, *171*, 9.
(33) Rodrigues, G. D.; da Silva, M. D. H.; da Silva, L. H. M.; Teixeira, L. D.; de Andrade, V. M. Liquid-Liquid Phase Equilibrium of Triblock Copolymer L64, Poly(ethylene oxide-b-propylene oxide-b-ethylene oxide), with Sulfate Salts from (278.15 to 298.15) K. *J. Chem. Eng. Data* **2009**, *54*, 1894.
(34) Martins, J. P.; da Silva, M. D. H.; da Silva, L. H. M.; Senra, T. D. A.; Ferreira, G. M. D.; Coimbra, J. S. D.; Minim, L. A. Liquid-Liquid Phase Equilibrium of Triblock Copolymer F68, Poly(ethylene oxide)-b-poly(propylene oxide)-b-poly(ethylene oxide), with Sulfate Salts. *J. Chem. Eng. Data* **2010**, *55*, 1618.
(35) Virtuoso, L. S.; Vello, K.; de Oliveira, A. A.; Junqueira, C. M.; Mesquita, A. F.; Lemes, N. H. T.; de Carvalho, R. M. M.; da Silva, M. C. H.; da Silva, L. H. M. Measurement and Modeling of Phase Equilibrium in Aqueous Two-Phase Systems: L35 plus Sodium Citrate plus Water, L35 Sodium Tartrate plus Water, and L35 plus Sodium Hydrogen Sulfite plus Water at Different Temperatures. *J. Chem. Eng. Data* **2012**, *57*, 462.
(36) Danson, S.; Ferry, D.; Alakhov, V.; Margison, J.; Kerr, D.; Jowle, D.; Brampton, M.; Halbert, G.; Ranson, M. Phase I dose escalation and pharmacokinetic study of pluronic polymer-bound doxorubicin (SP1049C) in patients with advanced cancer. *Br. J. Cancer* **2004**, *90*, 2085−2091.
(37) Singla, P.; Singh, O.; Sharma, S.; Betlem, K.; Aswal, V. K.; Peeters, M.; Mahajan, R. K. Temperature-Dependent Solubilization of the Hydrophobic Antiepileptic Drug Lamotrigine in Different Pluronic Micelles - A Spectroscopic, Heat Transfer Method, Small-Angle Neutron Scattering, Dynamic Light Scattering, and in Vitro Release Study. *ACS Omega* **2019**, *4*, 11251−11262.
(38) Yu, J.; Qiu, H.; Yin, S.; Wang, H.; Li, Y. Polymeric Drug Delivery System Based on Pluronics for Cancer Treatment. *Molecules* **2021**, *26*, 3610.
(39) Navi, M.; Abbasi, N.; Jeyhani, M.; Gnyawali, V.; Tsai, S. S. H. Microfluidic diamagnetic water-in-water droplets: a biocompatible cell encapsulation and manipulation platform. *Lab Chip* **2018**, *18*, 3361.
(40) Hasmann, F. A.; Santos, V. C.; Gurpilhares, D. B.; Pessoa-Junior, A.; Roberto, I. C. Aqueous two-phase extraction using thermoseparating copolymer: A new system for phenolic compounds removal from hemicellulosic hydrolysate. *J. Chem. Technol. Biotechnol.* **2008**, *83*, 167−173.
(41) Hespanhol, M. C.; Fontoura, B. M.; Quintão, J. C.; da Silva, L. H. M. Extraction and purification of gold from raw acidic electronic leachate using an aqueous biphasic system. *J. Taiwan Inst. Chem. Eng.* **2020**, *115*, 218.
(42) da Cunha, R. C.; Patrício, P. R.; Vargas, S. J. R.; da Silva, L. H. M.; da Silva, M. C. Hespanho. Green recovery of mercury from domestic and industrial waste. *J. Hazard. Mater.* **2016**, *304*, 417.
(43) Chagas, F. O.; Fontoura, B. M.; Vargas, S. J. R.; Da Silva, L. H. M.; Hespanhol, M. C. Liquid-Liquid Equilibrium Data of Macromolecule + Ammonium Thiosulfate + Water Ternary Systems at 283.2, 298.2, and 313.2 K. *J. Chem. Eng. Data* **2021**, *66*, 1011.
(44) Ghazizadeh Ahsaie, F.; Pazuki, G. Effect of carbohydrates, choline chloride based deep eutectic solvents and salts on the phase behavior of PEG-PPG copolymer ATPSs and partitioning of penicillin G. *J. Mol. Liq.* **2021**, *339*, 117152.
(45) Ahsaie, F. G.; Pazuki, G. Separation of phenyl acetic acid and 6-aminopenicillanic acid applying aqueous two-phase systems based on copolymers and salts. *Sci. Rep.* **2021**, *11*, 3489.
(46) Ebrahimi, A.; Pazuki, G.; Mozaffarian, M.; Ahsaie, F. G.; Abedini, H. Separation and Purification of C-Phycocyanin from Spirulina platensis Using Aqueous Two-Phase Systems Based on Triblock Thermosensitive Copolymers. *Food Bioprocess Technol.* **2023**, *16*, 2582−2597.
(47) Mohsen-Nia, M.; Rasa, H.; Modarress, H. Cloud-point measurements for (water + poly(ethylene glycol) + salt) ternary mixtures by refractometry method. *J. Chem. Eng. Data* **2006**, *51*, 1316−1320.
(48) Merchuk, J. C.; Andrews, B. A.; Asenjo, J. A. Aqueous two-phase systems for protein separation. *J. Chromatogr. B: Biomed. Sci. Appl.* **1998**, *711*, 285.
(49) Sosa, F. H. B.; de Araujo Sampaio, D.; Farias, F. O.; Bonassoli, A. B. G.; Igarashi-Mafra, L.; Mafra, M. R. Measurement and correlation of phase equilibria in aqueous two-phase systems containing polyethyleneglycol (2 000, 4 000, and 6 000) and sulfate salts (manganese sulfate and copper sulfate) at different temperatures (298.15, 318.15, and 338.15 K). *Fluid Phase Equilib.* **2017**, *449*, 68.
(50) Stragevitch, L.; D'Avila, S. G. Application of a generalized maximum likelihood method in the reduction of multicomponent liquid-liquid equilibrium data. *Braz. J. Chem. Eng.* **1997**, *14*, 41.
(51) Lo Nostro, P.; Ninham, B. W. Hofmeister phenomena: An update on ion specificity in biology. *Chem. Rev.* **2012**, *112*, 2286−2322.
(52) Kunz, W.; Henle, J.; Ninham, B. W. "Zur Lehre von der Wirkung der Salze" (about the science of the effect of salts): Franz Hofmeister's historical papers. *Curr. Opin. Colloid Interface Sci.* **2004**, *9*, 19.
(53) Zhang, Y.; Cremer, P. S. Interactions between macromolecules and ions: the Hofmeister series. *Curr. Opin. Chem. Biol.* **2006**, *10*, 658.
(54) Hebbeker, P.; Plamper, F. A.; Schneider, S. Effect of the Molecular Architecture on the Internal Complexation Behavior of Linear Copolymers and Miktoarm Star Polymers. *Macromol. Theory Simul.* **2015**, *24*, 110.
(55) Quintão, J. C.; Patrício, P. R.; Veloso, A. C. G.; de Carvalho, R. M. M.; da Silva, L. H. M.; Hespanhol, M. C. Liquid-liquid equilibrium of the ternary ammonium salt + poly(propylene glycol) + water system. *Fluid Phase Equilib.* **2017**, *442*, 96.
(56) Wang, Y.; Li, Y.; Han, J.; Xia, J.; Tang, X.; Chen, T.; Ni, L. Cloudy behavior and equilibrium phase behavior of triblock copolymer L64 + salt + water two-phase systems. *Fluid Phase Equilib.* **2016**, *409*, 439.
(57) Salamanca, M. H.; Merchuk, J. C.; Andrews, B. A.; Asenjo, J. A. On the kinetics of phase separation in aqueous two-phase systems. *J. Chromatogr. B: Biomed. Sci. Appl.* **1998**, *711*, 319.
(58) da Silva, L. H. M.; Loh, W. Calorimetric investigation of the formation of aqueous two-phase systems in ternary mixtures of water, poly(ethylene oxide) and electrolytes (or dextran). *J. Phys. Chem. B* **2000**, *104*, 10069.
(59) Titus, A. R.; Madeira, P. P.; Ferreira, L. A.; Chernyak, V. Y.; Uversky, V. N.; Zaslavsky, B. Y. Mechanism of Phase Separation in Aqueous Two-Phase Systems. *Int. J. Mol. Sci.* **2022**, *23*, 14366.
(60) Titus, A. R.; Ferreira, L. A.; Belgovskiy, A. I.; Kooijman, E. E.; Mann, E. K.; Mann, J. A.; Meyer, W. V.; Smart, A. E.; Uversky, V. N.; Zaslavsky, B. Y. Interfacial tension and mechanism of liquid-liquid phase separation in aqueous media. *Phys. Chem. Chem. Phys.* **2020**, *22*, 4574.

https://doi.org/10.1021/acs.jced.5c00298
J. Chem. Eng. Data 2025, 70, 3332−3343

(61) Hatti-Kaul, R. Aqueous two-phase systems: A general overview. *Appl. Biochem. Biotechnol., Part B* **2001**, *19*, 269−278.
(62) Watanabe, T.; Wang, Y.; Ono, T.; Chimura, S.; Isono, T.; Tajima, K.; Satoh, T.; Sato, S. I.; Ida, D.; Yamamoto, T. Topology and Sequence-Dependent Micellization and Phase Separation of Pluronic L35, L64, 10R5, and 17R4: Effects of Cyclization and the Chain Ends. *Polymers (Basel)* **2022**, *14*, 1823.
(63) Pérez-Sánchez, G.; Vicente, F. A.; Schaeffer, N.; Cardoso, I. S.; Ventura, S. P. M.; Jorge, M.; Coutinho, J. A. P. Rationalizing the Phase Behavior of Triblock Copolymers through Experiments and Molecular Simulations. *J. Phys. Chem. C* **2019**, *123*, 21224.
(64) de Lemos, L. R.; Santos, I. J. B.; Rodrigues, G. D.; Ferreira, G. M. D.; da Silva, L. H. M.; da Silva, M. D. H.; de Carvalho, R. M. M. Phase Compositions of Aqueous Two-Phase Systems Formed by L35 and Salts at Different Temperatures. *J. Chem. Eng. Data* **2010**, *55*, 1193.
(65) Rao, W.; Wang, Y.; Han, J.; Wang, L.; Chen, T.; Liu, Y.; Ni, L. Cloud Point and Liquid-Liquid Equilibrium Behavior of Thermosensitive Polymer L61 and Salt Aqueous Two-Phase System. *J. Phys. Chem. B* **2015**, *119*, 8201−8208.
(66) Hespanhol, M. C.; da Silva, L. H. M.; Fontoura, B. M.; de Andrade, V. M.; Mageste, A. B.; de Lemos, L. R. Phase Diagrams, Densities, and Refractive Indexes of Aqueous Two-Phase Systems Comprising (F68, L64, or PEO1500) + (Ammonium, Sodium, or Potassium Thiocyanate Salts) + Water: Effect of Cation and Type of Macromolecule. *J. Chem. Eng. Data* **2019**, *64*, 1991−1998.
(67) Renon, H.; Prausnitz, J. M. Local compositions in thermodynamic excess functions for liquid mixtures. *AIChE J.* **1968**, *14*, 135.
(68) Xavier, L.; Freire, M. S.; Vidal-Tato, I.; González-Álvarez, J. Application of aqueous two phase systems based on polyethylene glycol and sodium citrate for the recovery of phenolic compounds from Eucalyptus wood. *Maderas: Cienc. Tecnol.* **2015**, *17*, 0.
(69) Rodríguez-Salazar, N.; Valle-Guadarrama, S. Separation of phenolic compounds from roselle (Hibiscus sabdariffa) calyces with aqueous two-phase extraction based on sodium citrate and polyethylene glycol or acetone. *Sep. Sci. Technol.* **2020**, *55*, 2313.
(70) Friedman, M.; Jürgens, H. S. Effect of pH on the stability of plant phenolic compounds. *J. Agric. Food Chem.* **2000**, *48*, 2101−2110.
(71) Lapidot, T.; Harel, S.; Akiri, B.; Granit, R.; Kanner, J. PH-dependent forms of red wine anthocyanins as antioxidants. *J. Agric. Food Chem.* **1999**, *47*, 67.
(72) Padilha, C. E. d. A.; Nogueira, C. d. C.; Almeida, H. N.; Medeiros, W. R. D. B. d.; Oliveira Filho, M. A.; Araújo, J. S. d.; Santos, E. S. dos Separation and concentration of bioactive phenolic compounds by solvent sublation using three-liquid-phase system. *Food Bioprod. Process.* **2020**, *120*, 151.
(73) Santos, J. H. P. M.; Martins, M.; Silvestre, A. J. D.; Coutinho, J. A. P.; Ventura, S. P. M. Fractionation of phenolic compounds from lignin depolymerisation using polymeric aqueous biphasic systems with ionic surfactants as electrol ytes. *Green Chem.* **2016**, *18*, 5569.
(74) Willauer, H. D.; Huddleston, J. G.; Li, M.; Rogers, R. D. Investigation of aqueous biphasic systems for the separation of lignins from cellulose in the paper pulping process. *J. Chromatogr. B: Biomed. Sci. Appl.* **2000**, *743*, 127.
(75) Xavier, L.; Cabrera, M. N. Aqueous two-phase systems applied to the extraction of syringaldehyde and vanillin from eucalyptus wood residues. *Songklanakarin J. Sci. Technol.* **2021**, *43*, 153.
(76) Nagaraja, V. H.; Iyyaswami, R. Aqueous two phase partitioning of fish proteins: partitioning studies and ATPS evaluation. *J. Food Sci. Technol.* **2014**, *52*, 3539.
(77) Iqbal, M.; Tao, Y.; Xie, S.; Zhu, Y.; Chen, D.; Wang, X.; Huang, L.; Peng, D.; Sattar, A.; Shabbir, M. A. B.; Hussain, H. I.; Ahmed, S.; Yuan, Z. Aqueous two-phase system (ATPS): an overview and advances in its applications. *Biol. Proced. Online* **2016**, *18*, 18.
(78) Pereira, J. F. B.; Coutinho, J. A. P. *Em Handbooks in Separation Science*; Elsevier, 2020; Chapter 5.
(79) Lee, T. Y.; Chow, Y. H.; Chua, B. L. Application of aqueous micellar two-phase system for extraction of bioactive compounds. *AIP Conf. Proc.* **2019**, *2137*, 020007.
(80) Maia, A. M. M.; Pessoa-Junior, A.; Roberto, I. C. Extraction of hydroxycinnamic acids (ferulic and p-coumaric) from rice straw alkaline black liquor using Pluronic F-127 for potential applications in the cosmetics industry. *Ind. Crops Prod.* **2023**, *201*, 116914.

https://doi.org/10.1021/acs.jced.5c00298
J. Chem. Eng. Data 2025, 70, 3332−3343